

Microstructural Evolution of Cu-10at%C Nanocomposite Powder During High Energy Mechanical Milling

Wei Zeng^{a*}, DengShan Zhou^a, Deliang Zhang^a, Xiaoxia Li^b

^aThe State Key Laboratory of Metal Matrix Composites, School of Materials Science and Engineering, Shanghai Jiao Tong University, Room 303, Building C, 800 Dongchuan Road, Minhang District, Shanghai 200240, People's Republic of China

^bShanghai Fyntec Technology & Trading Co. Ltd, Room 1308, Building 1, 380 Tianyaoqiao Road, Xuhui District, Shanghai 200030, China

Received: September 6, 2015; Revised: October 5, 2015

The microstructural evolution of Cu-10at%C nanocomposite powder during high energy mechanical milling (HEMM) of Cu/graphite powder mixture was studied. It was found that the efficiency of milling in refining the microstructure of the copper matrix was very high with the presence of graphite in the Cu/graphite powder mixture. The average grain size of the Cu matrix reaches its minimum value of about 30 nm just after milling for 6 h, and the graphite particles were refined down to about 10~20 nm after milling for 24 h. It envisaged that the refining of graphite particles down to 10 nm would be accompanied by formation of nanograins of copper matrix, and it appears that high energy mechanical milling can greatly enhance the solubility of carbon in copper though it is very hard to determine the exact solubility.

Keywords: *high energy mechanical milling (HEMM), nanocomposite, Cu-graphite, microstructural evolution*

1. Introduction

High energy mechanical milling (HEMM) is one of those advanced techniques to synthesize amorphous alloy powders, nanocrystalline powder and nanocomposite powder¹ and has been employed to the alloying of immiscible systems such as Cu-Cr^[2], Cu-Nb^[3], Cu-Fe^[4], Ag-Cu^[5]. By consolidation of the mechanically milled powders, one can obtain ultrafine grained materials with high strength, good ductility and high thermal stability⁶⁻⁸. The ability of tremendously enhancing the solid solubility of one component in another is one of the major effects of HEMM⁹. In this study, our focus is on the microstructural evolution of Cu-10at%C nanocomposite during HEMM, where the equilibrium solid solubility of carbon in copper is virtually zero¹⁰. HEMM of Cu-graphite composite powders have been studied by several groups¹¹⁻¹⁵. The pioneering studies of Saji et al.¹¹ and Yamane et al.¹² on mechanical milling of copper-graphite mixtures with different weight ratio of graphite indicated the solubility of carbon in copper can be as high as 28.5at%, while the study carried out by Marque et al.¹³ on mechanical milled Cu-10at%C composite showed that the carbon content was overestimated by the former researchers and the existence of carbon nanoparticles was shown. Transmission electron microscopy examination confirmed that the microstructure of the mechanically milled Cu-10at%C nanocomposite consisted of nanostructured copper matrix dispersed with carbon nanoparticles¹⁴. While these studies mainly focus on the carbon solubility in copper achieved by HEMM, the microstructural evolution of copper-graphite nanocomposite

powders need to be clarified with more details. Our study on HEMM of the Cu-10at%C composite, with the carefully chosen milling times, showed that the efficiency of HEMM in refining the copper matrix was so high that 6 h of milling can result in formation of a nanocrystalline copper matrix with average grain size of about 30 nm. The fast formation of nanocrystalline copper matrix dramatically influenced the formation of carbon nanoparticles with sizes of 10~20 nm through the assistance of the large area of grain boundaries to enhance the diffusion and solubility of carbon in copper.

2. Experimental Procedure

A Cu-10at%C nanocomposite powder was prepared by HEMM with pure copper powder (99.9wt% pure, particle size: <45 μm , -325 mesh) and TIMCAL natural graphite powder (99.9wt% pure, particle size: 40~55 μm) in a QM-3SP4 planetary ball mill operated at 500 rpm. The mill container was charged with 100 g of copper and graphite powder mixture with a composition of 10at%C and 500 g hardened steel balls (diameter: 16 mm) under an argon atmosphere, the ball-to-powder ratio was 5:1. The powder was taken out for characterization after milled for 1 h, 3 h, 6 h, 10 h, 15 h and 24 h. The milled powder samples were analyzed by using X-ray diffractometry (XRD) using Cu K α radiation (Rigaku, Ultima IV). The lattice parameter of copper in the milled powder particles was calculated with the least-square method using {111}, {200}, {220}, {311}, {222} and {400} peaks, and the weighted function was $\cos^2\theta/\sin\theta + \cos^2\theta/\theta$.

*e-mail: zengwei@sjtu.edu.cn

The copper grain size of the milled powders were estimated using Williamson-Hall¹⁶ equation:

$$B \cos \theta = 0.89 \lambda / D + \varepsilon \sin \theta \quad (1)$$

Where B is the full width at half maximum (FWHM) of a diffraction peak at a Bragg angle of 2θ of copper, λ is the wavelength of the X-ray used, D is the average crystallite size which is considered to be the grain size, ε is the internal elastic strain of the crystalline lattice, the XRD profiles were refined using pseudo-voigt function before calculation.

Samples for scanning electron microscopy (SEM) (FEI, Sirion 200) examination were mounted in resin and polished with diamond polish agent down to 0.5 μm and further polished using silica suspension with particle size about 50 nm, Vickers microhardness measurements were performed on the polished cross sections of the powder particles mounted in resin with a load of 0.098 N (10 g) and loading time of 10 s. The milled powder particles were also examined using transmission electron microscopy (TEM) (JEOL JEM2010), with the TEM specimens being prepared by embedding the powder particles in resin and thinning the powder particle/resin composite by grinding and ion milling (Gatan ion mill, Model 691).

3. Results

Figure 1 shows the XRD patterns of Cu-10at%C powder mixture and Cu-10at%C nanocomposite powders milled for different times. As shown in Figure 1, the XRD pattern of the as-blended Cu-10at%C powder presents the diffraction peaks of graphite (0002) and cuprite Cu_2O (111). The cuprite may be formed during the atomization of copper to make the Cu powder used in this study. After milling for only 1 h, the diffraction peak of graphite disappeared and the Cu_2O peak could not be distinguished after 3 h of milling. It was thought that the disappearance of the graphite diffraction peak indicates the dissolution of carbon in copper matrix¹¹, and the Cu_2O oxide layer might be broken down during milling resulting in disappearance of the Cu_2O peak.

With further milling, the peaks of Cu shifted to slightly lower angle, indicating the increase in the lattice parameter of Cu matrix. The change of the lattice parameter of Cu matrix with increasing milling time is shown in Figure 2. The lattice parameter of Cu remains nearly unchanged before milling for 6 h, and increases sharply after milled for 6 h and then reaches its ultimate value. The increase of the lattice parameter of Cu indicates the formation of Cu(C) solid solution^{11-13,15}. Thus, after milled for 6 h, the concentration of carbon in Cu increases with the increase of milling time, and reaches its saturation milled for 24 h.

As the broadening and weakening of the XRD peaks of Cu matrix indicate the decrease of Cu grain sizes with increasing milling time, calculation using Williamson-Hall equation can well estimate the grain size of copper. Figure 3 shows the change of calculated average grain size of the Cu matrix with increasing milling time. As shown in Figure 3, just after milling for 6 h, the average grain size of the Cu matrix was reduced to about 30 nm, and at the same time, the lattice parameter starts to increase, it can be proposed

that the formation of the Cu(C) solid solution should be accomplished by the formation of copper nanograins.

To illustrate the evolution of graphite particles, SEM was performed as shown in Figure 4a, after 1 h of milling, the graphite particles were embedded in the copper matrix

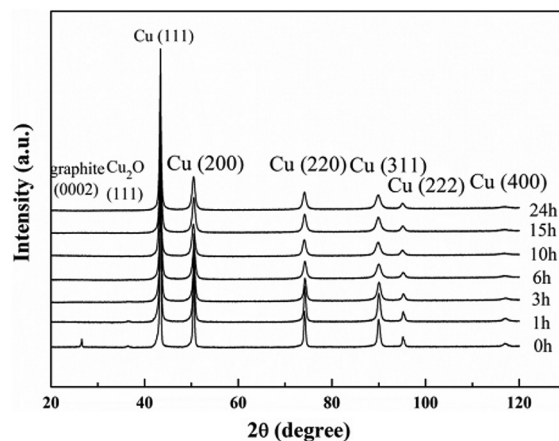


Figure 1. XRD patterns of the powders milled for 0 h, 1 h, 3 h, 6 h, 10 h, 15 h and 24 h respectively.

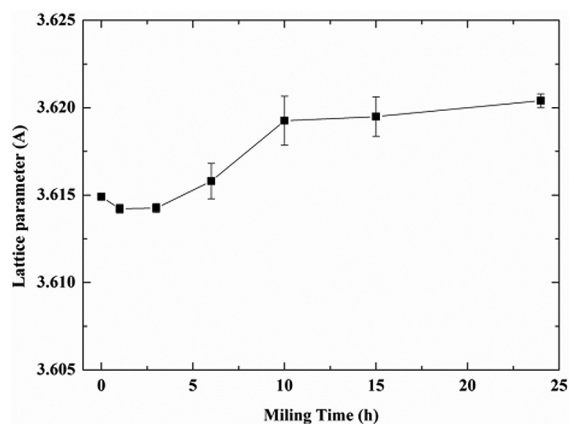


Figure 2. Change of lattice parameter of Cu matrix as a function of milling time.

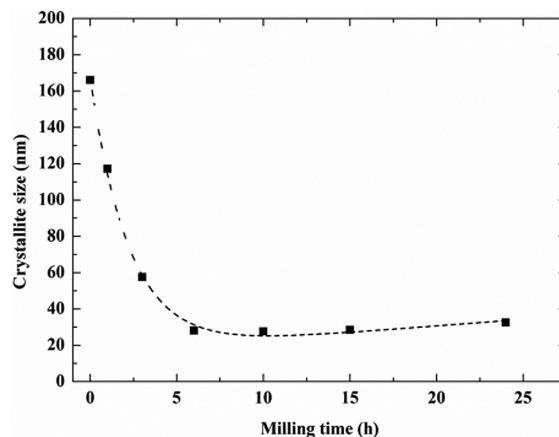


Figure 3. Grain size of Cu matrix versus milling time.

and mainly distributed at the boundaries between deformed copper ribbons. As shown in Figure 4b, after milling for 6 h, large graphite particles can hardly be seen, and the fine graphite particles were homogeneously distributed in the matrix. Elongated graphite particles free regions were also visible in the microstructure. With further increasing the milling time to 24 h, the graphite particles were further refined and became hardly visible in the SEM backscattered electron images, as shown in Figure 4c. EDX analysis was also performed to confirm the carbon distribution in powder milled for 1 h as shown in Figure 4d, the carbon concentration was high at the boundaries between deformed copper ribbons and no carbon could be detected in copper region, which indicates no Cu(C) solid solution formed.

While XRD calculation of grain size may be inaccurate sometimes, direct TEM observation was carried out. Figure 5 shows the TEM bright field image of the microstructures of powder particles milled for 6 h and 24 h respectively. As shown in Figure 5a, after 6 h of milling, the grain sizes of the Cu

matrix were in the range of 20~40 nm, in agreement with the average crystallite size of 30 nm determined based on the XRD pattern of the powder, thus the grain size of copper determined from Williamson-Hall method was considered to be accurate. The light contrast regions marked with arrows were determined to be amorphous carbon¹⁴. As shown in Figure 5b, the microstructure of the 24 h milled powder particles was quite similar to that of the 6 h milled powder particles. This indicates that increasing milling time beyond 6 h does not produce a significant change of the microstructure.

Corresponding to the microstructural evolution of the Cu-10at%C nanocomposite, Figure 6 shows the change of the microhardness of the Cu-10at%C nanocomposite powder particles with increasing milling time. The microhardness reached its maximum value about 200 HV after milling for 6 h which is consistent with the grain refinement into nano region indicating the strengthening of Cu-carbon nanocomposite is mainly ascribed to the grain refinement.

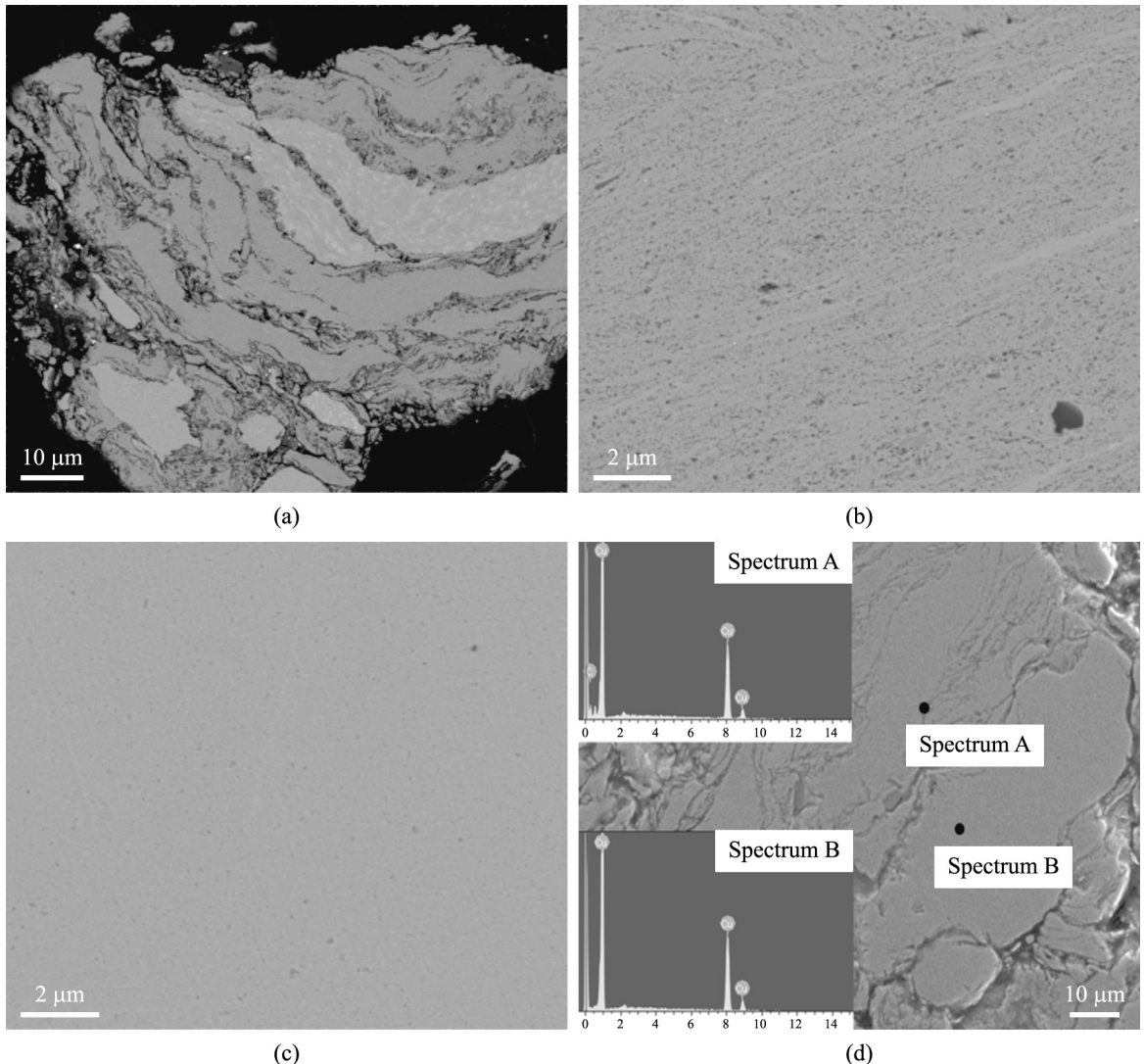


Figure 4. SEM backscattering electron images of powder particles milled for (a) 1 h, (b) 6 h, (c) 24 h (d) energy dispersive X-ray (EDX) analysis of powder milled for 1 h.

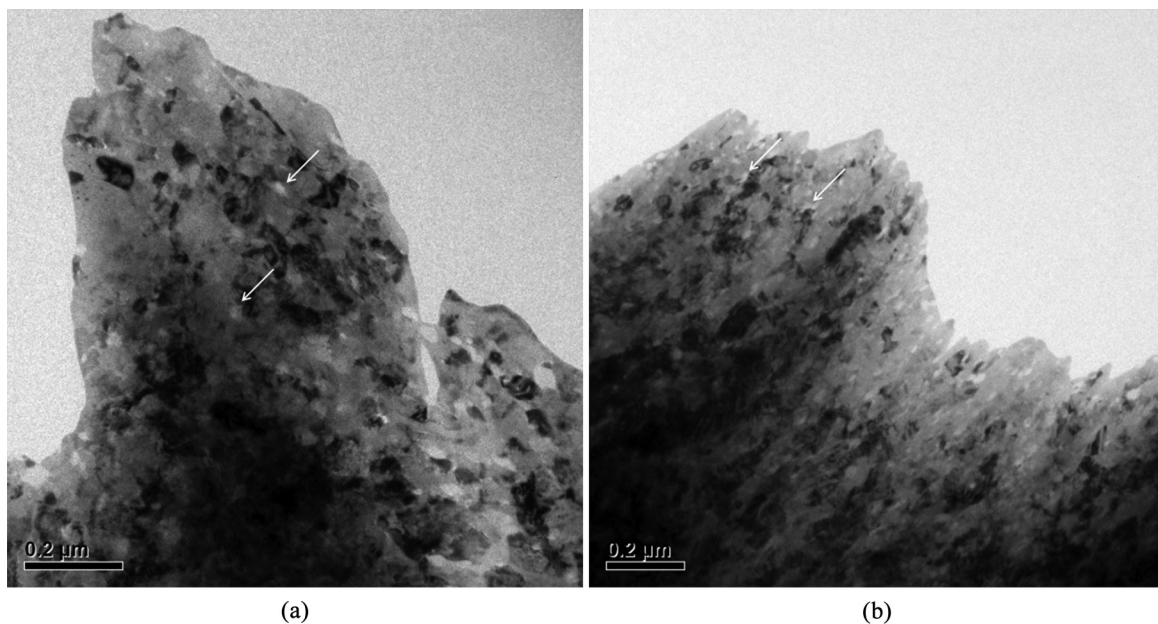


Figure 5. TEM bright field images of the microstructures of powder particles milled for (a) 6 h and (b) 24 h. The white nanoparticles such as those indicated by the white arrows in the images are carbon nanoparticles.

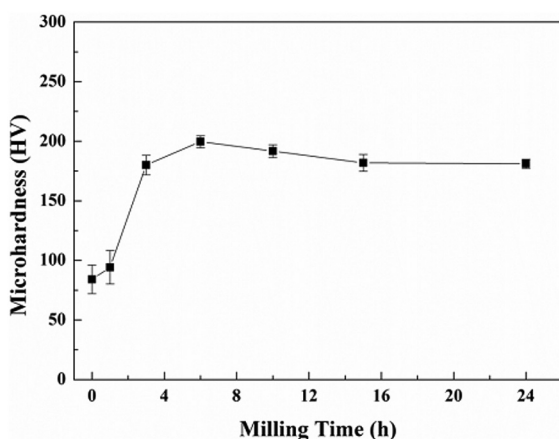


Figure 6. Change of microhardness of the Cu-10at%C nanocomposite powder particles versus milling time.

4. Discussion

Based on the microstructural characterization of the milled Cu-10at%C nanocomposite powder particles shown above, the microstructural evolution of the powder particles during HEMM can be divided into three stages involving the interaction of copper grains and graphite nanoparticles.

In stage 1, the refining of copper matrix grains dominates. Graphite is usually used as perfect lubricant due to the fact that it can be easily exfoliated by shear force. During HEMM of Cu-10at%C powder blending of composite powder, the graphite particles are easily exfoliated and the copper particles are easily deformed, thus the graphite particles are adsorbed onto the deformed copper ribbons preventing over cold welding of them. This enhances the efficiency of HEMM in plastically deforming the powder particles and refining the copper grains. Copper can be easily deformed

as well as cold welded during milling, as the presence of graphite was absorbed onto the deformed copper ribbon surface with short milling time, as shown in Figure 4a. With further milling, the copper ribbons were heavily deformed and the graphite particles were crushed into smaller particles, thus the refining of both copper grain size and graphite particles size happened, as shown in the microstructure of Figure 4b and Figure 4c. The reduction of grain size is due to localization of plastic deformation in the form of shear bands containing a high density of dislocations, formation of subgrains or cells by annihilation of dislocations and the conversion of subgrains and cells into grains through mechanically driven grain rotation and subgrain boundary sliding¹. But, at this time, the copper grain size is not fine enough for the diffusion of carbon to occur because of the limited solid solution of carbon in copper⁴, thus no solid solution forms.

Once the grains of copper matrix are refined to 30 nm, things become different, and the process enters stage 2. In this stage, the concentration of carbon in copper increases with increasing milling time. As shown above, the formation of Cu(C) solid solution coincides with formation of nanocrystalline copper during HEMM. With milling shorter than 6 h, the lattice parameter remains nearly unchanged, which strongly indicates the lattice parameter of copper will not increase unless the grain size of copper is small enough. Meanwhile, the increase of lattice parameter of copper is the result of the formation of Cu(C) solid solution, thus the formation of Cu(C) need the assistant of nanocrystalline copper grains, and after milling for longer enough, the lattice parameter reaches a saturated value. Two mechanisms may be involved in this phenomenon. One mechanisms is that the large area of non-equilibrium grain boundaries in the nanocrystalline copper greatly enhances the diffusion of carbon along the grain boundaries and provides extra free energy to the system

to raise it to a sufficiently high level to drive the formation of non-equilibrium Cu(C) solid solution. The other mechanism is that the energy input during HEMM results in the refinement of the microstructure of the Cu-10at%C nanocomposite as well as heat resulting in an increase in the temperature of powder, which can lead to a higher solid solubility of carbon in copper and high diffusion coefficient. Though both these two mechanisms contribute to the formation of Cu(C) solid solution, the one associated with grain boundary diffusion and free energy may dominate.

Stage 3 contains the formation of carbon nanoparticles. Conventional X-ray diffraction methods are of limited sensitivity to short range inhomogeneities or ordering¹⁷. This difficulty happens in determining the true solubility of carbon in copper, since Cu-C is an immiscible system and there might be short range inhomogeneities in the Cu(C) solid solution. To determine the carbon content in the Cu(C) solid solution based on lattice parameter, we use the correlation between the carbon content and the lattice parameter of FCC Fe (C) solid solution which can be treated as being similar to the Cu(C) solid solution due to the high similarity between the lattice parameters of FCC Fe and FCC Cu. It was reported that dissolution of 1at% of C can result in 0.168% lattice expansion of FCC Fe^[18]. Based on this, we can infer that about 1at% of C is dissolved in Cu. This means that 90% of carbon in the Cu-10at%C is still in the form of carbon nanoparticles. Even though, it is true that the solid solubility of carbon in copper was dramatically enhanced through HEMM.

References

- Zhang DL. Processing of advanced materials using high-energy mechanical milling. *Progress in Materials Science*. 2004; 49(3):537-560. [http://dx.doi.org/10.1016/S0079-6425\(03\)00034-3](http://dx.doi.org/10.1016/S0079-6425(03)00034-3).
- Gerasimov KB, Mytnichenko SV and Pavlov SV. Microstructure of the products of mechanical alloying in the Cu-Cr system. *Doklady Physical Chemistry*. 1996; 351(1-3):310-312.
- Botcharova E, Heilmaier M, Freudenberger J, Drew G, Kudashov D, Martin U, et al. Supersaturated solid solution of niobium in copper by mechanical alloying. *Journal of Alloys and Compounds*. 2003; 351(1):119-125. [http://dx.doi.org/10.1016/S0925-8388\(02\)01025-3](http://dx.doi.org/10.1016/S0925-8388(02)01025-3).
- Eckert J, Holzer JC, Krill CE III and Johnson WL. Mechanically driven alloying and grain size changes in nanocrystalline Fe-Cu powders. *Journal of Applied Physics*. 1993; 73(6):2794-2802. <http://dx.doi.org/10.1063/1.353055>.
- Uenishi K, Kobayashi KF, Ishihara KN, Shingu PH. Formation of a super-saturated solid solution in the Ag-Cu system by mechanical alloying. *Materials Science and Engineering: A*. 1991; 134:1342-1345.
- Botcharova E, Freudenberger J and Schultz L. Mechanical and electrical properties of mechanically alloyed nanocrystalline Cu-Nb alloys. *Acta Materialia*. 2006; 54(12):3333-3341. <http://dx.doi.org/10.1016/j.actamat.2006.03.021>.
- Morris DG and Morris MA. Microstructure and strength of nanocrystalline copper alloy prepared by mechanical alloying. *Acta Metallurgica et Materialia*. 1991; 39(8):1763-1770. [http://dx.doi.org/10.1016/0956-7151\(91\)90144-P](http://dx.doi.org/10.1016/0956-7151(91)90144-P).
- Darling KA, Roberts AJ, Mishin Y, Mathaudhu SN and Kecskes LJ. Grain size stabilization of nanocrystalline copper at high temperatures by alloying with tantalum. *Journal of Alloys and Compounds*. 2013; 573:142-150. <http://dx.doi.org/10.1016/j.jallcom.2013.03.177>.
- Suryanarayana C. Mechanical alloying and milling. *Progress in Materials Science*. 2001; 46(1-2):1-184. [http://dx.doi.org/10.1016/S0079-6425\(99\)00010-9](http://dx.doi.org/10.1016/S0079-6425(99)00010-9).
- Hansen M, Anderko K and Salzberg HW. Constitution of binary alloys. *Journal of the Electrochemical Society*. 1958; 105(12):260C-261C. <http://dx.doi.org/10.1149/1.2428700>.
- Saji S, Kadokura T, Anada H, Notoya K, Takano N. Solid solubility of carbon in copper during mechanical alloying. *Materials Transactions, JIM(Japan)*. 1998; 39(7):778-781.
- Yamane T, Okubo H, Hisayuki K, Oki N, Konishi M, Komatsu M, et al. Solid solubility of carbon in copper mechanically alloyed. *Journal of Materials Science Letters*. 2001; 20(3):259-260. <http://dx.doi.org/10.1023/A:1006701708039>.
- Marques MT, Correia JB and Conde O. Carbon solubility in nanostructured copper. *Scripta Materialia*. 2004; 50(7):963-967. <http://dx.doi.org/10.1016/j.scriptamat.2004.01.016>.
- Carvalho PA, Fonseca I, Marques MT, Correia JB and Vilar R. Transmission electron microscopy study of copper-carbon nanocomposite. *Materials Science and Technology*. 2006; 22(6):673-678. <http://dx.doi.org/10.1179/174328406X84058>.
- Liu X, Liu Y and Xu R, An J and Zhanyi C. Fabrication of the supersaturated solid solution of carbon in copper by mechanical alloying. *Materials Characterization*. 2007; 58(6):504-508. <http://dx.doi.org/10.1016/j.matchar.2006.06.022>.

5. Conclusions

The microstructural evolution of a Cu-10at%C nanocomposite during HEMM was investigated. The results show that the microstructural evolution process can be divided into three stages:

Stage 1: the refining of copper matrix to 30 nm, while the exfoliation of graphite into small particles happens, but no Cu(C) solid solution was formed

Stage 2: carbon starts diffusion into copper matrix forming the Cu(C) solid solution

Stage 3: the concentration of carbon in copper reaches its limit and the residual carbon particles were refined into carbon nanoparticles with sizes in the range of 10~20 nm.

The microhardness of the Cu-10at%C nanocomposite increases to its maximum value about 200 HV after milling for 6 h when the grain size is refined to its minimum value about 30 nm, indicating grain boundary strengthening was the major strengthening mechanism.

Acknowledgements

Funding from Ministry of Science and Technology, China through a 973 project on the scientific basis of fabrication of advanced metal matrix composites (No. 2012CB619600) and from the National Natural Science Foundation of China (Project approval No. 51271115) is gratefully acknowledged.

16. Williamson GK and Hall WH. X-ray line broadening from fided aluminium and wolfram. *Acta Metallurgica*. 1953; 1(1):22-31. [http://dx.doi.org/10.1016/0001-6160\(53\)90006-6](http://dx.doi.org/10.1016/0001-6160(53)90006-6).
17. Ma E. Alloys created between immiscible elements. *Progress in Materials Science*. 2005; 50(4):413-509. <http://dx.doi.org/10.1016/j.pmatsci.2004.07.001>.
18. Hummelshøj TS, Christiansen TL and Somers MAJ. Lattice expansion of carbon-stabilized expanded austenite. *Scripta Materialia*. 2010; 63(7):761-763. <http://dx.doi.org/10.1016/j.scriptamat.2010.05.031>.